# Rotation-invariant optical recognition of three-dimensional objects

José J. Esteve-Taboada, Javier García, and Carlos Ferreira

An automatic method for rotation-invariant three-dimensional (3-D) object recognition is proposed. The method is based on the use of 3-D information contained in the deformed fringe pattern obtained when a grating is projected onto an object's surface. The proposed method was optically implemented by means of a two-cycle joint transform correlator. The rotation invariance is achieved by means of encoding with the fringe pattern a single component of the circular-harmonic expansion derived from the target. Thus the method is invariant for rotations around the line of sight. The whole experimental setup can be constructed with simple equipment. Experimental results show the utility of the proposed method. © 2000 Optical Society of America

*OCIS codes:* 100.4550, 100.6890, 100.5760.

## 1. Introduction

Most of the existing methods for pattern recognition through optical correlation have been developed for bidimensional (2-D) objects. The most frequently used optical correlators have been the VanderLugt optical correlator[1] and the joint transform correlator (JTC).[2] These systems are not invariant to any parameter except lateral shifts of the input object, which allows targets at different locations within an image to be processed simultaneously. Other invariant properties could be obtained by use of harmonic decompositions, such as circular harmonics (CH) for rotation invariance,[3] Mellin radial harmonics or logarithmic radial harmonics for 2-D scale invariance,[4,5] logarithmic harmonics for one-dimensional scale invariance,[6] or even deformation harmonics for other distortion properties.[7] In these methods the input object is decomposed into a set of orthogonal harmonic functions (except for logarithmic radial harmonics), and the reference function is chosen as a single expansion order. This approach provides invariant pattern recognition at the cost of a lower discrimination than that obtained with the conventional methods, because here the reference function is only a single term out of the full harmonic decomposition.

Nevertheless, in spite of the usefulness of 2-D pattern recognition, there are applications in which the object information is not contained in just one 2-D projection but in its entire three-dimensional (3-D) shape.[8,9] Thus a full 3-D treatment is required. In the past few years much research has been devoted to the task of optical recognition of 3-D objects. A first possibility is to use optical or digital processing over a range image.[10,11] However, the main drawback of this setup is the need for a range camera, which is not readily available. A different approach uses a JTC architecture combined with electronic processing of the images obtained from several cameras.[12,13] This is a complex setup and requires a considerable amount of digital calculation. Other techniques are based on holography as a method for recording 3-D information.[14–16] They are based on correlating the planar holograms of the 3-D functions. A practical difficulty with these procedures is that a hologram from a rough object is determined by the microscopic structure of the object surface, producing a low correlation for two similar 3-D objects that have a different microscopic structure.

Recently, a real-time optical technique for the recognition of 3-D objects was proposed.[17] The process relies on using Fourier transform profilometry (FTP)[18] for introducing the 3-D information into the system. FTP is based on projecting a grating onto an object surface and capturing a 2-D image of the scene with a CCD camera. The obtained 2-D image

The authors are with the Departament Interuniversitari d'Òptica, Facultat de Física, Universitat de València, c/Doctor Moliner 50, 46100 Burjassot, València, Spain. J. J. Esteve-Taboada's e-mail address is jose.j.esteve@uv.es.

Received 2 February 2000; revised manuscript received 21 June 2000.

0003-6935/00/325998-08$15.00/0

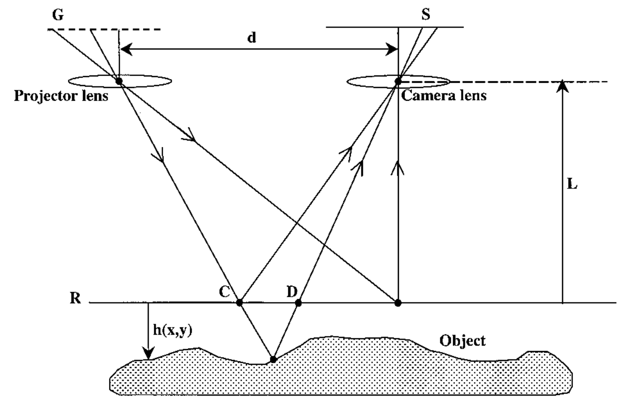

Fig. 1. Optical arrangement for projecting the grating and grabbing the 2-D images.

is a deformed grating pattern that carries information on the depth and the shape of the object. Since the deformed fringe pattern obtained with the fringe projection technique carries information about the complete shape of the object, the analysis of such patterns is the basis of the method for recognizing 3-D objects.

In this paper we propose a system that permits optical rotation-invariant 3-D object recognition. It combines the FTP technique, CH decomposition, and a real-time recognition setup based on the JTC architecture.

In Section 2 we review the main aspects of the FTP method and the 3-D JTC introduced in Ref. 17 that are relevant for our purposes. In Section 3 we provide the necessary details of CH decomposition. In Section 4 a description of the method is presented. In Section 5 optical experiments show the performance of the method introduced here. Finally, in Section 6, the main conclusions are outlined.

## 2. Fourier Transform Profilometry Method and Three-Dimensional Object Recognition

The FTP method for obtaining the 3-D shape of an object is based on projecting a grating on its surface and capturing a 2-D image with a camera.[18] If the axes of the projector and the camera are not coincident, a distorted fringe pattern that encodes the 3-D object information is obtained. In our experiment we employ the geometry shown in Fig. 1, in which the optical axes of the projector and the camera lie in the same plane and are parallel. Let us consider a reference plane R, which is a fictitious plane that serves as a reference from which the object height $h(x, y)$ is measured. The slide projector forms the conjugate image of the grating G on plane R. The reference plane is imaged onto sensor plane S by the camera lens. Following Ref. 17, for a general object with varying $h(x, y)$ the deformed grating image, grabbed by the camera, expressed in terms of its Fourier components is given by

$$s(x, y) = r(x, y) \sum_{n=-\infty}^{\infty} q_n(x, y)\exp(2\pi i n f_0 x), \qquad (1)$$

where

$$q_n(x, y) = A_n \exp[in\phi(x, y)], \qquad (2)$$

$f_0$ being the fundamental frequency of the observed grating image, $r(x, y)$ the reflectivity distribution on the object surface [$r(x, y)$ is zero outside the object extent] and $\phi(x, y) = 2\pi f_0 \overline{CD}$, where $\overline{CD}$ is defined in Fig. 1. Each of the diffraction orders of the deformed grating has a spatial carrier frequency $nf_0$, is modulated in phase through $n\phi(x, y)$, and has an overall amplitude modulation of $r(x, y)$.

The phase $\phi(x, y)$ contains the information about the 3-D shape, since the connection between $\phi(x, y)$ and the height of the object $h(x, y)$ can be written as

$$\phi(x, y) = \frac{-2\pi f_0 d h(x, y)}{L - h(x, y)}. \qquad (3)$$

In particular, if $L \gg h(x, y)$ it is clear that the phase is just proportional to the height of the object.

This phase function can be digitally obtained following the method depicted in Fig. 2. Let us assume a 3-D input object described by its height $h(x, y)$ [see Fig. 2(a)]. Consider that a regular grating pattern is projected onto this 3-D object and a that 2-D image is taken with a camera. A distorted grating pattern that carries information about the 3-D shape of the object is obtained [see Fig. 2(b)]. This 2-D image has the amplitude given by Eqs. (1) and (2). The 2-D Fourier transform (FT) of the function $s(x, y)$ may be written as

$$\tilde{s}(u, v) = \left[\sum_{n=-\infty}^{\infty} Q_n(u - nf_0, v)\right] \otimes \mathscr{F}[r(x, y)], \quad (4)$$

where the symbol $\otimes$ denotes the convolution operation and $Q_n(u, v)$ represents the FT of $q_n(x, y)$.

Assuming that $r(x, y)$ and $\phi(x, y)$ vary slowly compared with the frequency $f_0$ of the grating pattern, all the spectra $Q_n(u - nf_0, v)$ are separated from one other according the carrier frequency $f_0$ [see Fig. 2(c)]. Thus, using a mask, one can easily filter these spectra and select only the spectrum with $n = 1$. To simplify, we take as the origin of coordinates the position of the first diffraction order, obtaining [see Fig. 2(d)]

$$\tilde{s}'(u, v) = Q_1(u, v) \otimes \mathscr{F}[r(x, y)]. \qquad (5)$$

The object height information can be obtained as an encoded phase modulation with an inverse FT of Eq. (5):

$$\mathscr{F}^{-1}[\tilde{s}'(u, v)] = A_1 r(x, y)\exp[i\phi(x, y)]. \qquad (6)$$

This expression describes a complex image. As an example, Fig. 2(e) depicts this image separating amplitude and phase information for the object shown in Fig. 2(a). As stated above, the phase contains the object height information, whereas the amplitude is just the reflectivity of the object. Therefore we have encoded the 3-D object in this complex image. In the following the function derived as explained above and given by Eq. (6) will be denoted PEHF (phase-

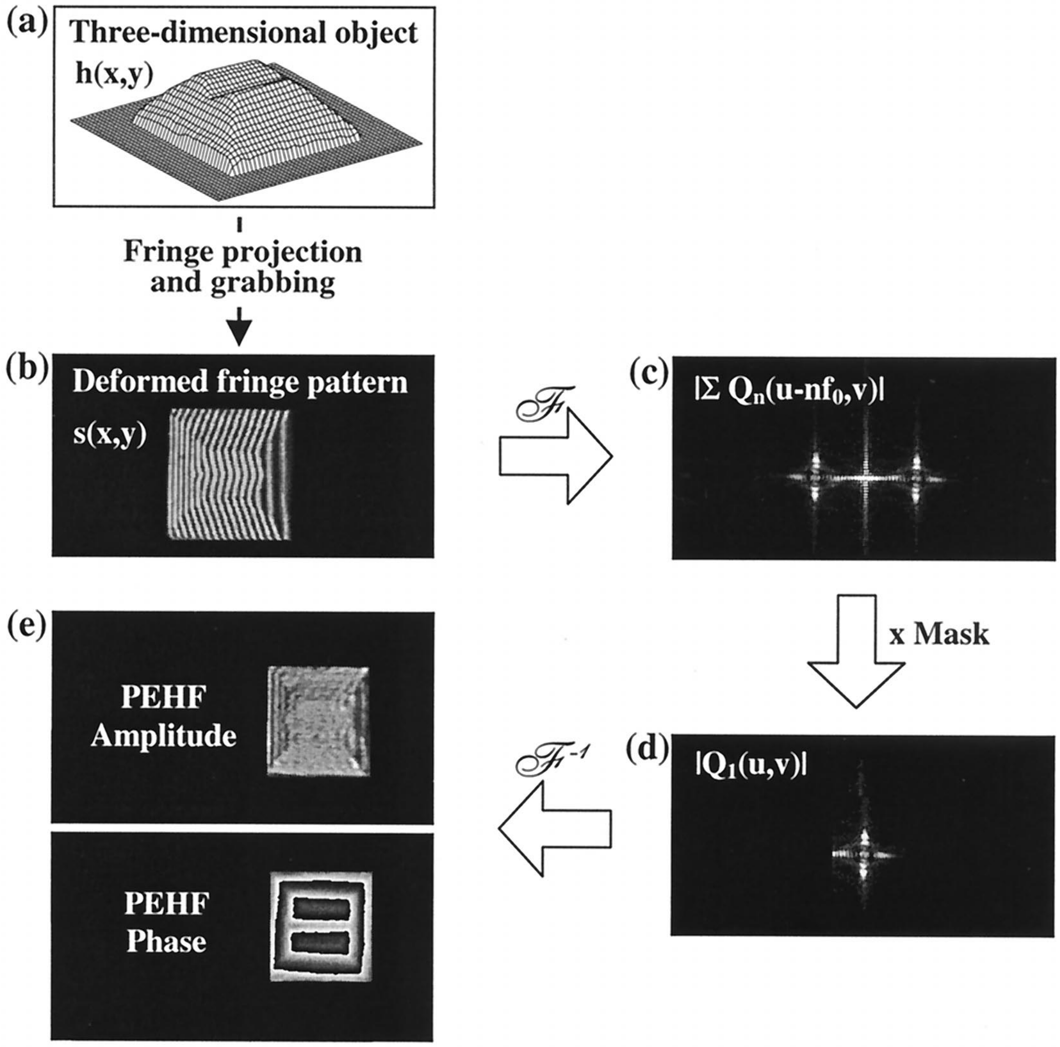


Fig. 2. Scheme of the procedure for obtaining the object-height information by fringe projection.

encoded height function). Since the phase calculation by computer gives principal values ranging from $-\pi$ to $\pi$, the phase distribution is wrapped into this range and consequently has discontinuities with $2\pi$-phase jumps for variations more than $2\pi$. These discontinuities could be corrected with any of the conventional unwrapping techniques (see, for instance, Refs. 19 and 20).

The 3-D object recognition can be obtained by means of encoding the 3-D input objects into PEHF's and correlating them. Esteve-Taboada *et al.* implemented this method in Ref. 17, using a modified JTC setup. The outline of the method is as follows: The joint input plane is prepared with the scene to be analyzed and the target, both obtained by means of projecting fringes onto the 3-D objects and grabbing the result as 2-D images. After performing a FT, in the first diffraction order we have the joint spectrum of the PEHF's corresponding to the objects in the input plane. Taking the intensity of this first order and retransforming, we obtain the correlation between the PEHF's that correspond to the input objects. This permits 3-D object recognition by means of correlating PEHF's.

## 3. Circular-Harmonic Decomposition

The CH expansion is used for rotation-invariant pattern recognition.[3] An input object expressed in polar coordinates $f(r, \theta)$ can be analyzed into a set of orthogonal functions as

$$f(r, \theta) = \sum_{M=-\infty}^{\infty} f_M(r)\exp(iM\theta), \tag{7}$$

where

$$f_M(r) = \frac{1}{2\pi}\int_0^{2\pi} f(r, \theta)\exp(-iM\theta)\mathrm{d}\theta, \tag{8}$$

$M$ being the expansion order.

As is well known, a filter matched to only one term of the CH expansion provides rotation-invariant pat-

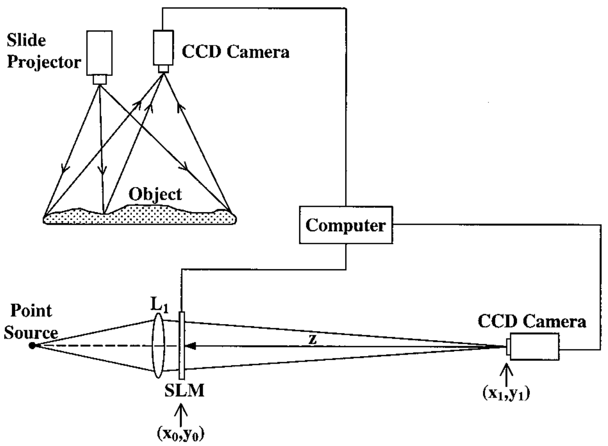


Fig. 3. Experimental setup including the acquisition part and the JTC process.

tern recognition. A target rotated by an angle $\alpha$ can be expressed as

$$f(r, \theta + \alpha) = \sum_{M=-\infty}^{\infty} f_M(r)\exp(iM\alpha)\exp(iM\theta). \quad (9)$$

With a single harmonic $g(r, \theta) = f_M(r)\exp(iM\theta)$ out of the CH expansion of $f(r, \theta)$ as a reference function, the correlation with the rotated target at the origin of the correlation plane is given by

$$C_M(\alpha) = 2\pi \exp(iM\alpha) \int_0^{\infty} |f_M(r)|^2 r\mathrm{d}r. \quad (10)$$

Thus if we use only one component of the CH expansion as reference function, as the phase factor $\exp(iM\alpha)$ is removed when we take the intensity of the correlation plane, the result is independent of the angular orientation of the target, and rotation invariance is achieved. In contrast, the simultaneous use of several harmonics destroys the correlation peak as a result of the different values of the phase factors.

Considering that the CH expansion involves a coordinate transformation of the target into polar coordinates, the functional dependence of the target varies with the origin of the polar coordinate system. This origin is known as the CH expansion center. The choice of an adequate expansion center will ensure good performance of the filter. There are several methods to select this CH expansion center.[21–23] In our experiment we used the method proposed in Ref. 23, which ensures good discrimination capability of the filter.

Once the expansion center has been chosen, the CH component, $g(r, \theta) = f_M(r)\exp(iM\theta)$, is sampled in Cartesian coordinates. For its later use we will refer to the CH component in Cartesian coordinates as $g_c(x, y)$.

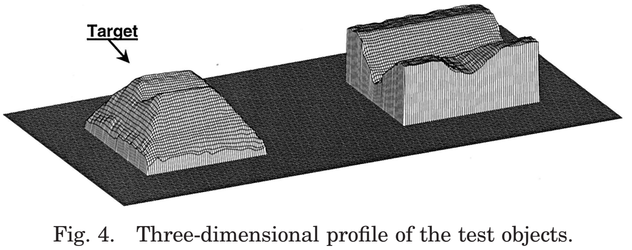


Fig. 4. Three-dimensional profile of the test objects.

## 4. Description of the Method

The proposed method of rotation-invariant recognition is based on the theory introduced in Ref. 17 and on the well-known property of the CH expansion to obtain rotation-invariant pattern recognition. The theory developed in Ref. 17 is based on using a JTC. In a conventional JTC it is necessary to place the scene to be analyzed and the target side by side in the input plane. In the method proposed here the joint input image is composed of the deformed fringe patterns of the objects to be tested and of a CH component that acts as a reference function that carries part of the target's 3-D information. This reference function is the CH component of the PEHF obtained from the target. Thus, using the 3-D JTC introduced in Ref. 17, we will obtain the correlation between the PEHF's that correspond to the objects in the input scene and the CH component of the target's PEHF.

It is important to note that a CH component is complex (except for the zero expansion order), that is, has phase as well as amplitude information. Thus one cannot use a simple transparency at the input plane. One possibility is to treat the real and the imaginary parts of a CH function as two separate positive reference objects in a JTC setup.[24] Another approach consists of encoding phase and amplitude through a computer-generated hologram with Lohmann's detour phase method.[25,26]

In our proposal we encode the complex CH component information, performing digitally the interference of this CH component with the plane wave $A \times \exp(-i2\pi y/p)$, where $p$ has been chosen to be equal to the period of the grating projected onto the objects. Assuming that we have chosen the CH component of order $M$, $g_c(x, y)$, the interference pattern is

$$\begin{aligned} |g_c(x, y) + A \exp(-i2\pi y/p)|^2 &= |g_c(x, y)|^2 + A^2 \\ &\quad + 2A|g_c(x, y)| \cos[\varphi(x, y) - 2\pi y/p] \\ &= |g_c(x, y)|^2 + A^2 + g_c^*(x, y)A \exp(-i2\pi y/p) \\ &\quad + g_c(x, y)A \exp(i2\pi y/p), \end{aligned} \quad (11)$$

where $\varphi(x, y)$ is the phase of $g_c(x, y)$. It is clear that the pattern consists of fringes of period $p$ and a local phase difference given by $\varphi(x, y)$. For obtaining an interference with a good contrast we have taken an amplitude $A$ of the plane wave that equals the maximum of the absolute value of the complex CH component. The interference function so obtained has a nonzero background level, but this will not be important in our case, since we will filter the Fourier plane and will consider only the first diffraction order. Furthermore, this filtering will remove all terms in

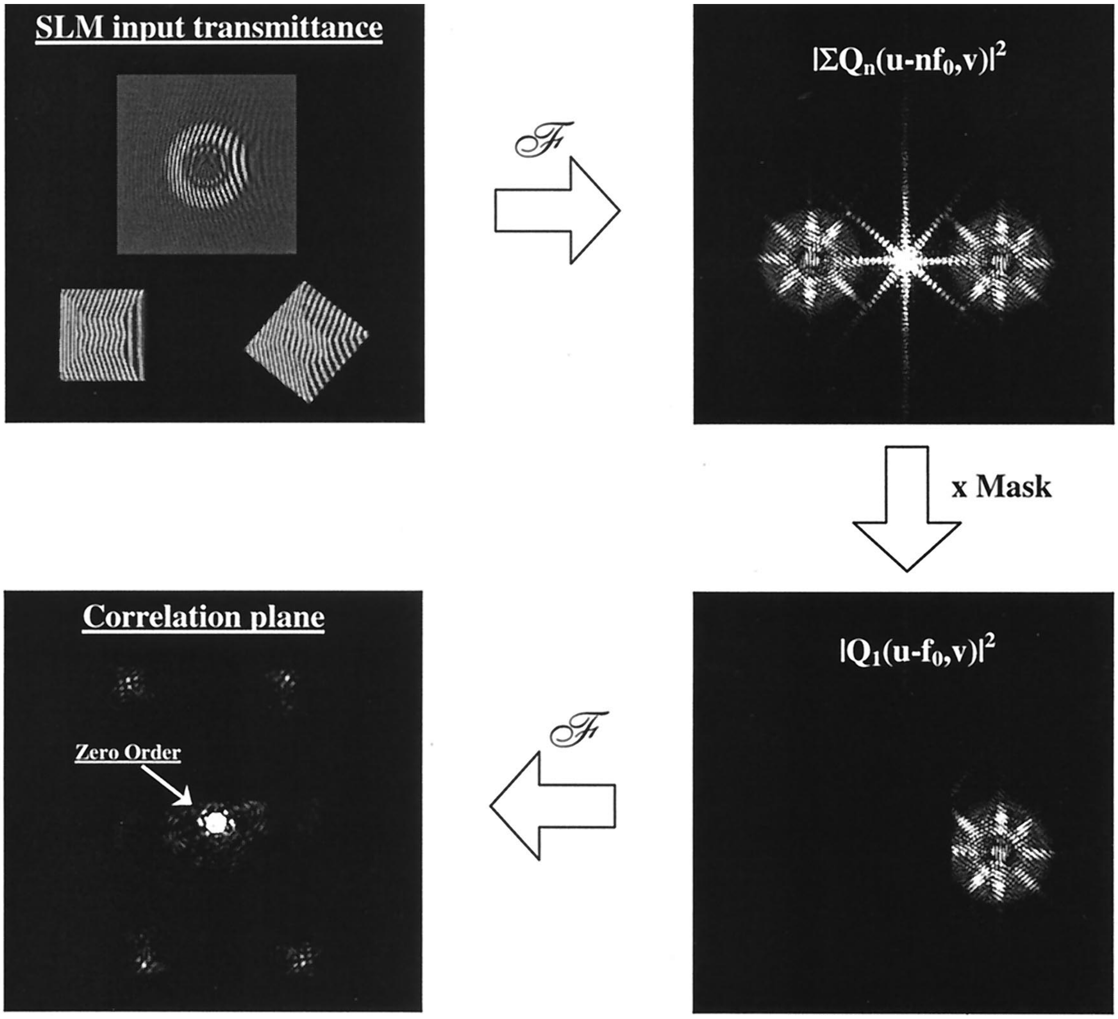


Fig. 5. Whole experimental process using the two-cycle modified JTC.

Eq. (11) except for the final one, which contains the CH component.

In summary, in the first diffraction order of the FT of the input plane we obtain the superposition of the FT of the PEHF's of the input objects and the FT of the CH that acts as the reference function. Grabbing the intensity and performing a new FT, we finally obtain the correlation between the PEHF's and the CH.

## 5. Optical Experiments

The usefulness of the proposed method was tested by optical experiments. The actual setup is the one shown on Fig. 3. A slide projector is used to image a Ronchi grating of 8 lines/mm onto the objects' surface. The objects are two 3-D pieces placed on a black uniform plane that serves as a reference from which object heights are compared. One of the pieces is the target, whereas the other serves to test the discrimination capability of the system. The deformed grating patterns are recorded by a Pulnix Model TM-765 CCD camera. By performing the process shown in Fig. 2 by computer we can obtain the phase functions that correspond to the object's height information. Figure 4 shows a perspective view of one 3-D input scene obtained with this procedure. In this figure we indicate which is the 3-D object that acts as the target. The footprint of the objects is 4 cm $\times$ 3.5 cm, and the maximum object height is 2 cm. Note that the 3-D reconstruction was performed only for graphic purposes.

In an initial stage previous to the correlation we obtain the PEHF from the target (following the process shown in Fig. 2), and from this function we calculate the CH component. For the target we chose a CH component of order $M = 4$. As stated above, the CH expansion center is selected by the method proposed in Ref. 23.

We prepared two scenes. The first one is used to test the rotation-invariant feature of the system. To prepare it, we projected fringes onto two targets, one rotated 45° with respect to the other, and we took a 2-D image with the CCD camera. We calculated the $M = 4$ CH component of the PEHF corresponding to the target. We encoded with fringes this CH component with the suitable grating period, and the result was added to the image of the targets. The joint input scene, which is fed into the spatial light mod-

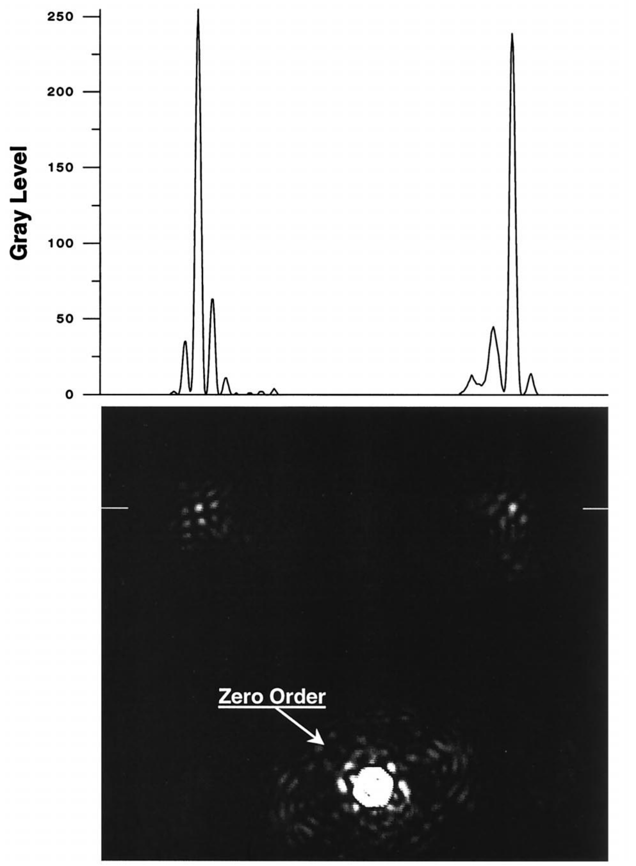


Fig. 6. Experimental optical correlation for the scene shown in the upper left-hand image of Fig. 5. This image shows only the upper part of the JTC output and the zero order. A horizontal profile along the position marked with the narrow white lines is shown.

ulator (SLM), is shown in the upper left-hand image of Fig. 5. This image is stored in a frame grabber memory as a $800 \times 600$ pixel image and is sent to the SLM at the plane $(x_0, y_0)$ of the optical setup (see Fig. 3). The SLM is a liquid-crystal screen obtained from a Sony Model VPL-S500 video projector. $L_1$ is a 300-mm-focal-length achromatic doublet.

With a second Pulnix CCD camera, without a lens, the intensity of the first order at plane $(x_1, y_1)$ is obtained. This image is sent to the SLM again. Therefore, as is demonstrated in Ref. 17, in this new cycle of the modified JTC we have finally, at plane $(x_1, y_1)$, correlation terms in three different positions. In the optical axis (zero order) we obtain the addition of the autocorrelation terms, in the upper part of the image we obtain the correlation between the PEHF's of the input objects and the CH component of the target's PEHF, and in the lower part we obtain the same distribution except for a mirror reflection. This output plane is captured again with a CCD camera, so the intensity of this distribution is recorded. The whole experimental process using the two-cycle modified JTC is presented in Fig. 5. Figure 6 shows the experimentally obtained intensity output plane when the input scene is the one shown in the upper left-hand image of Fig. 5. This figure shows only the upper part of the JTC output and the zero order. In addition, a horizontal profile over the position marked with the narrow white lines is shown. This correlation output takes into account the information about the similarity of the 3-D shape of the objects. We can observe two high correlation peaks, owing to the targets that appear in this first scene.

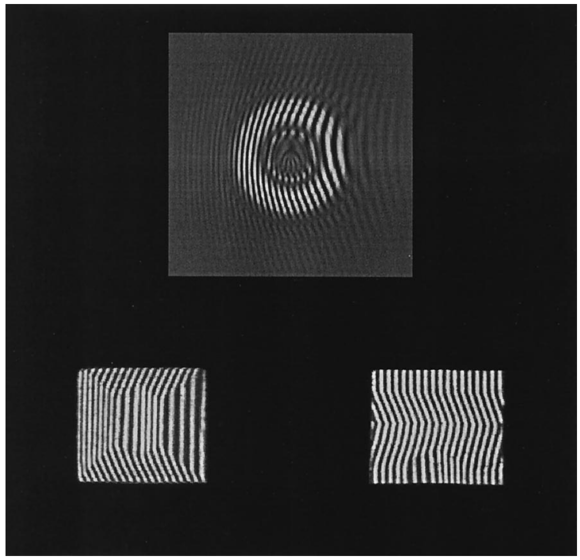

Fig. 7. Input scene used to test the discrimination capability of the system. It is composed of the target (rotated this time 90° with respect to the object on the left in the upper left-hand image of Fig. 5) and of another object that, while having the same 2-D contour as the target, has a different 3-D shape.

The second scene is used to test the discrimination capability of the system. We projected fringes onto the target (rotated this time 90° with respect to the object on the left-hand side in the previous scene) and on another object, which, although it has the same 2-D contour as the target, has a different 3-D shape. We added to this image the same fringe-modulated CH component as in the previous scene. The resulting image is shown in Fig. 7. Performing the same process as with the previous scene, we obtain the correlation output. This experimental output plane, captured with a CCD camera, is shown in Fig. 8. We can observe a high correlation peak, owing to the target that appears in this second scene. The correlation peak corresponding to the other object, which should appear on the left-hand side, has a negligible intensity. Obviously this correlation output allows for excellent discrimination, which permits recognition of the 3-D target.

It is worth noting that, if the discrimination were not so high, further enhancement of the experimental correlation peaks would be possible (see, for example, image-processing algorithms or nonlinear processing applied to the Fourier domain in Refs. 27 and 28, respectively).

Finally, note that, if the camera and the projector are far from the object, i.e., $L \gg h(x, y)$, the phase $\phi(x, y)$ is directly proportional to the height of the

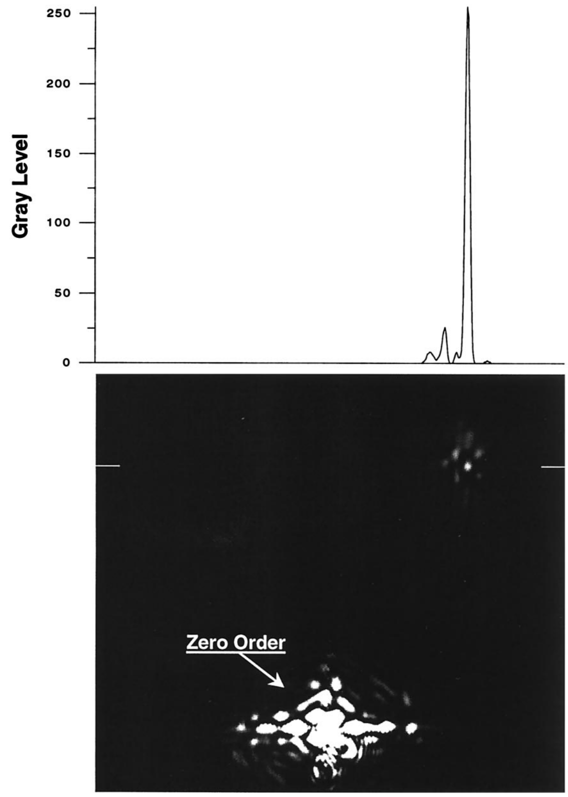


Fig. 8. Experimental optical correlation for the scene shown in Fig. 7. This image shows only the upper part of the JTC output and the zero order. A horizontal profile along the position marked with the narrow white lines is shown.

object [see Eq. (3)]; then the experimental setup sketched in Fig. 3 is also invariant to shifts along the direction given by $h(x, y)$ [see Ref. (17)]. This allows for detection that is invariant under displacements on the three axes and under rotations of the target.

## 6. Conclusions

We have presented a method for achieving rotation-invariant 3-D object recognition. The method is based on using the 3-D information contained in the deformed fringe pattern obtained when a grating is projected onto the object's surface. When this deformed fringe pattern is analyzed, the first order of its Fourier series expansion contains the object's height information encoded on the phase. Therefore taking the intensity of the first diffraction order permits the realization of a two-cycle modified JTC recognition process, in which the input objects are the distorted patterns that contain the 3-D shape of the objects with a phase-encoded height.

The proposed method has been optically implemented with CH decomposition, thus achieving the rotation-invariant property. We are now studying other decomposition sets to obtain other invariant properties. From linear correlation our system inherits the invariance to translations in a plane perpendicular to the line of sight; moreover, as stated above, under certain conditions our setup is also invariant to shifts along the direction given by the height of the object.

Experimental results verify the derived theory and show the utility of the method introduced here. The whole experimental setup can be constructed with simple equipment, and, except for the grabbing of the images and the *a priori* computation of the CH component, there is no need for electronic or digital processing. As a consequence, the system is simple and robust. Moreover, once the CH component derived from the target has been calculated, the system can operate at nearly video rates, and both the reference function and the input scene can be rapidly changed to scan different filters or input objects. The robustness and the simplicity of the optical setup are in contrast with other procedures of 3-D object recognition.

In principle our system presents some limitations, mainly derived from FTP, such as limited inspected volume, given by the depth of focus of both the projector and the camera, and the long distance requirement for obtaining detection invariance along the line of sight. These disadvantages can be reduced with, for example, an interference system for generating the grating and a telecentric camera lens.

Possible applications of our system are in automatic vision, such as classification, testing, and tracking of 3-D objects. The system described in this paper in its present form is specially designed for dealing with small objects (typically of a few centimeters). Nevertheless, it is easy to extend it to large objects.

José J. Esteve-Taboada acknowledges a grant from the Conselleria de Cultura, Educació i Ciència (Generalitat Valenciana). This study was supported by Spanish Ministerio de Educación y Cultura project PB96-1134-C02-02.

### References

1. A. VanderLugt, "Signal detection by complex spatial filtering," IEEE Trans. Inf. Theory **IT-10,** 139–145 (1964).
2. C. S. Weaver and J. W. Goodman, "A technique for optically convolving two functions," Appl. Opt. **5,** 1248–1249 (1966).
3. Y. N. Hsu and H. H. Arsenault, "Optical pattern recognition using circular harmonic expansion," Appl. Opt. **21,** 4016–4019 (1982).
4. D. Mendlovic, E. Marom, and N. Konforti, "Shift and scale invariant pattern recognition using Mellin radial harmonics," Opt. Commun. **67,** 172–176 (1988).
5. J. Rosen and J. Shamir, "Scale invariant pattern recognition with logarithmic radial harmonic filters," Appl. Opt. **28,** 240–244 (1989).
6. D. Mendlovic, N. Konforti, and E. Marom, "Shift and projection invariant pattern recognition using logarithmic harmonics," Appl. Opt. **29,** 4784–4789 (1990).
7. E. Marom, D. Mendlovic, and N. Konforti, "Generalized spatial deformation harmonic filter for distortion invariant pattern recognition," Opt. Commun. **78,** 416–424 (1990).
8. O. Faugeras, *Three-Dimensional Computer Vision. A Geometric Viewpoint* (MIT Press, Cambridge, Mass., 1993).
9. A. Pu, R. Denkewalter, and D. Psaltis, "Real-time vehicle navigation using a holographic memory," Opt. Eng. **36,** 2737–2746 (1997).

10. E. Paquet, M. Rioux, and H. H. Arsenault, "Invariant pattern recognition for range images using the phase Fourier transform and a neural network," Opt. Eng. **34,** 1178–1183 (1995).
11. E. Paquet, P. García-Martínez, and J. García, "Tridimensional invariant correlation based on phase-coded and sine-coded range images," J. Opt. **29,** 35–39 (1998).
12. J. Rosen, "Three-dimensional electro-optical correlation," J. Opt. Soc. Am. A **15,** 430–436 (1998).
13. J. Rosen, "Three-dimensional joint transform correlator," Appl. Opt. **37,** 7538–7544 (1998).
14. T. Poon and T. Kim, "Optical image recognition of three-dimensional objects," Appl. Opt. **38,** 370–381 (1999).
15. T. Kim and T. Poon, "Extraction of 3-D location of matched 3-D object using power fringe-adjusted filtering and Wigner analysis," Opt. Eng. **38,** 2176–2183 (1999).
16. B. Javidi and E. Tajahuerce, "Three-dimensional object recognition by use of digital holography," Opt. Lett. **25,** 610–612 (2000).
17. J. J. Esteve-Taboada, D. Mas, and J. García, "Three-dimensional object recognition by Fourier transform profilometry," Appl. Opt. **38,** 4760–4765 (1999).
18. M. Takeda and K. Mutoh, "Fourier transform profilometry for the automatic measurement of 3-D object shapes," Appl. Opt. **22,** 3977–3982 (1983).
19. M. Takeda, H. Ina, and S. Kobayashi, "Fourier-transform method of fringe-pattern analysis for computer-based topography and interferometry," J. Opt. Soc. Am. **72,** 156–160 (1982).
20. D. C. Ghiglia and L. A. Romero, "Robust two-dimensional weighted and unweighted phase unwrapping that uses fast transforms and iterative methods," J. Opt. Soc. Am. A **11,** 107–117 (1994).
21. Y. Sheng and H. H. Arsenault, "Method for determining expansion centers and predicting sidelobe levels for circular harmonic filters," J. Opt. Soc. Am. A **4,** 1793–1797 (1987).
22. G. Prémont and Y. Sheng, "Fast design of circular harmonic filters using simulated annealing," Appl. Opt. **32,** 3116–3121 (1993).
23. P. García-Martínez, J. García, and C. Ferreira, "A new criterion for determining the expansion center for circular-harmonic filters," Opt. Commun. **117,** 399–405 (1995).
24. F. T. S. Yu, X. Li, E. Tam, S. Jutamulia, and D. A. Gregory, "Rotation invariant pattern recognition with a programmable joint transform correlator," Appl. Opt. **28,** 4725–4727 (1989).
25. D. Mendlovic, E. Marom, and N. Konforti, "Complex reference-invariant joint-transform correlator," Opt. Lett. **15,** 1224–1226 (1990).
26. A. W. Lohmann and D. P. Paris, "Binary Fraunhofer holograms generated by computer," Appl. Opt. **6,** 1739–1748 (1967).
27. M. Alam and Y. Gu, "Sobel operator based multiobject joint transform correlation," Optik (Stuttgart) **100,** 28–32 (1995).
28. B. Javidi, "Nonlinear joint power spectrum based optical correlation," Appl. Opt. **28,** 2358–2367 (1989).